Input Catalogue for Space-VLBI Phase-referencing

Yoshiharu Asaki (ISAS)
Aug 9, 2002

Abstract

An input catalogue for space-VLBI phase-referencing has been made using an image simulator which has been developed for this work. An example of the input catalogue and the following statistical analysis are mentioned in this report.

1 Introduction

Phase-referencing (P-R) by means of the antenna nodding method is considered to be a promising technique for future space-VLBI (SVLBI) missions to obtain higher sensitivities. The effectiveness of P-R will depend on weather conditions, separation angles between target and reference sources, observing frequencies, slew rates of radio telescopes which limit the achievable switching cycle time, and so on. The most important factors for P-R are the existence of a reference source very close to the target, and the switching cycle time: if a suitable reference cannot be found the P-R will not work at all, and the faster the switching cycle time is, the better the effectiveness will be.

Switching the spacecraft attitude with a cycle time of less than a few minutes with an positional accuracy much less than the HPBW of the space radio telescope (SRT) will be hard to achieve. Since spacecraft have limitations on the mass and power budgets, we will not be able to prepare an attitude control system for fast switching. To consider the trade-off between these budgets and the effectiveness of P-R, we have to investigate the dependency of the effectiveness on the switching cycle time as well as the probability that a reference source can be found close to an arbitrary target source.

In this work the following approach is adopted to discuss the effectiveness of P-R instead of investigating the probability of the existence of a reference source:

(i) Scientifically interesting pairs of sources are selected for P-R observations.

(ii) The effectiveness for each pair of sources is evaluated.

(iii) Statistical studies are applied to the effectiveness of the selected pairs.

To conduct the first and third items, an input catalogue for SVLBI P-R has been made using an image simulator which has been developed for this work. Assumed observing conditions for SVLBI P-R is mentioned in section2. An example of the input catalogue for weak GPS sources is shown in section 3. A statistical analysis about the catalogue is described in section 4. An appendix gives a description about the image simulator for SVLBI P-R.

2 Assumptions of the Observing Conditions

The effectiveness of P-R is dependent on the observing conditions very much. The following observing conditions are considered to evaluate the effectiveness of P-R in SVLBI, though some of them contribute to make more optimistic situation:

(i) All the sources listed are assumed to be completely point-like ones. The assumed flux densities of the reference sources are referred to correlated flux densities at 8 GHz, or total flux densities at 5 GHz because almost all the flux densities at higher frequencies cannot be investigated easily.

(ii) Observations using the VLBA and two spacecraft are demonstrated. To evaluate the SNR of the brightness peaks of the targets, only space-ground baselines are considered because we are interested in how much P-R improves the sensitivities of baselines with an SRT whose sensitivity is low.

(iii) The astronomical radio seeing demonstrated listed in Table **??** in Appendix **??** is applied.

(iv) Maximum observing time is 14 hours while the total number of samples in (u, v) depends on the declination and separation angle of the sources.

(v) The switching cycle time is fixed to 120 sec independent of the separation angles. The on-source duration (pre-vector-average duration) is fixed to 10 sec.

(vi) The SNR of the target without P-R is calculated in the continuous observation. The pre-vector-averaging duration is fixed to 10 sec.

(vii) No weighting function and no deconvolution in imaging are considered. Simple 2-D Fourier transformation is just applied in making synthesis maps.

3 Input Catalogue for the P-R SVLBI

reference sources:

$*$: VLBA calibrator source

† : ICRF source

‡ : correlated flux density at 8 GHz

§ : total flux density at 5 GHz

effectiveness:

◯ : P-R is useful.

△ : P-R is not needed although the brightness peak is obtained at the phase tracking center, because the obtained SNR with P-R is not improved so much comparing with the continuous observation.
(You have to note that the total number of samples in (u, v) is 1/12 smaller than that of the continuous observation.)

× : P-R is not useful.

3.1 Weak GPS Sources

3.1.1 1525+6801

	flux density (SNR)			separation angle
	X	Ka	Q	
1525+6801	30mJy (72.3)	10mJy (4.4)	8mJy (4.3)	(target)
J1526+6650*	0.312Jy	0.312Jy‡	0.312Jy‡	1.01°
J1459+7140†	3.733Jy§	3.733Jy§	3.733Jy§	4.45°
1525+6801 – J1526+6650				
	X	Ka	Q	
SNR after P-R	53.9	3.9	3.7	
effectiveness	△	×	×	
1525+6801 – J1459+7140				
	X	Ka	Q	
SNR after P-R	54.6	4.0	3.8	
effectiveness	△	×	×	

3.1.2 1538+5920

	flux density (SNR)			separation angle
	X	Ka	Q	
1538+5920	35mJy (65.4)	15mJy (3.6)	10mJy (3.1)	(target)
J1551+5806*	0.305Jy	0.305Jy‡	0.305Jy‡	1.94°
J1603+5730*	0.312Jy	0.312Jy‡	0.312Jy‡	3.61°
J1604+5714*	0.491Jy	0.491Jy‡	0.491Jy‡	3.83°
J1510+5702†	0.264Jy	0.264Jy‡	0.264Jy‡	4.44°
1538+5920 – J1551+5806				
	X	Ka	Q	
SNR after P-R	54.3	6.9	4.1	
effectiveness	△	◯	×	
1538+5920 – J1603+5730				
	X	Ka	Q	
SNR after P-R	51.1	3.4	4.4	
effectiveness	△	×	×	
1538+5920 – J1604+5714				
	X	Ka	Q	
SNR after P-R	50.8	4.4	4.4	
effectiveness	△	×	×	
1538+5920 – J1510+5702				
	X	Ka	Q	
SNR after P-R	51.5	3.9	3.9	
effectiveness	△	×	×	

3.1.3 1551+6822

	flux density (SNR)			separation angle
	X	Ka	Q	
1551+6822	25mJy (73.6)	6mJy (4.6)	2mJy (3.5)	(target)
J1526+6650*	0.312Jy	0.312Jy‡	0.312Jy‡	2.79°
J1623+6624*	0.287Jy	0.287Jy‡	0.287Jy‡	3.50°
J1642+6856†	1.526Jy§	1.526Jy§	1.526Jy§	4.62°
1551+6822 – J1526+6650				
	X	Ka	Q	
SNR after P-R	55.5	3.9	3.5	
effectiveness	△	×	×	
1551+6822 – J1623+6624				
	X	Ka	Q	
SNR after P-R	55.7	3.8	4.2	
effectiveness	△	×	×	
1551+6822 – J1642+6856				
	X	Ka	Q	
SNR after P-R	53.7	3.1	4.1	
effectiveness	△	×	×	

3.1.4 1557+6220

	flux density (SNR)			separation angle
	X	Ka	Q	
1557+6220	25mJy (63.9)	6mJy (3.3)	2mJy (5.2)	(target)
J1551+5806*	0.305Jy	0.305Jy‡	0.305Jy‡	4.15°
1557+6220 – J1551+5806				
	X	Ka	Q	
SNR after P-R	45.9	4.0	3.8	
effectiveness	△	×	×	

3.1.5 1600+7131

	flux density (SNR)			separation angle
	X	Ka	Q	
1600+7131	30mJy (74.8)	8mJy (3.5)	2mJy (3.6)	(target)
J1531+7206*	0.231Jy	0.231Jy‡	0.231Jy‡	2.38°
J1459+7140†	3.733Jy§	3.733Jy§	3.733Jy§	4.86°
J1642+6856†	1.526Jy§	1.526Jy§	1.526Jy§	4.28°
1600+7131 – J1531+7206				
	X	Ka	Q	
SNR after P-R	57.2	3.8	3.9	
effectiveness	△	×	×	
1600+7131 – J1459+7140				
	X	Ka	Q	
SNR after P-R	54.6	3.6	4.1	
effectiveness	△	×	×	
1600+7131 – J1642+6856				
	X	Ka	Q	
SNR after P-R	59.2	3.8	3.7	
effectiveness	△	×	×	

3.1.6 1622+6630

	flux density (SNR)			separation angle
	X	Ka	Q	
1622+6630	210mJy (70.8)	100mJy (12.3)	50mJy (3.5)	(target)
J1623+6624*	0.287Jy	0.287Jy‡	0.287Jy‡	0.05°
J1629+6757*	0.224Jy	0.224Jy‡	0.224Jy‡	1.71°
J1642+6856†	1.526Jy§	1.526Jy§	1.526Jy§	3.15°
1622+6630 – J1623+6624				
	X	Ka	Q	
SNR after P-R	69.2	45.7	3.8	
effectiveness	△	◯	×	
1622+6630 – J1629+6757				
	X	Ka	Q	
SNR after P-R	70.3	45.9	4.0	
effectiveness	△	◯	×	
1622+6630 – J1642+6856				
	X	Ka	Q	
SNR after P-R	67.0	41.1	3.2	
effectiveness	△	◯	×	

3.1.7 1642+6701

	flux density (SNR)			separation
	X	Ka	Q	angle
1642+6701	35mJy (65.9)	18mJy (3.7)	10mJy (3.7)	(target)
J1623+6624*	0.287Jy	0.287Jy‡	0.287Jy‡	1.98°
J1629+6757*	0.224Jy	0.224Jy‡	0.224Jy‡	1.58°
J1642+6856†	1.526Jy§	1.526Jy§	1.526Jy§	2.01°
J1700+6830*	0.377Jy	0.377Jy‡	0.377Jy‡	2.30°
J1716+6836*	0.829Jy	0.829Jy‡	0.829Jy‡	3.61°
1642+6701 – J1623+6624				
	X	Ka	Q	
SNR after P-R	61.3	7.6	3.2	
effectiveness	△	◯	×	
1642+6701 – J1629+6757				
	X	Ka	Q	
SNR after P-R	61.2	5.2	5.3	
effectiveness	△	◯	×	
1642+6701 – J1642+6856				
	X	Ka	Q	
SNR after P-R	59.6	8.2	3.4	
effectiveness	△	◯	×	
1642+6701 – J1700+6830				
	X	Ka	Q	
SNR after P-R	60.8	5.2	4.2	
effectiveness	△	◯	×	
1642+6701 – J1716+6836				
	X	Ka	Q	
SNR after P-R	60.0	5.5	3.7	
effectiveness	△	◯	×	

3.1.8 1819+6707

	flux density (SNR)			separation
	X	Ka	Q	angle
1819+6707	90mJy (62.2)	35mJy (4.5)	25mJy (3.7)	(target)
J1842+6809†	0.932Jy§	0.932Jy§	0.932Jy§	2.39°
1819+6707 – J1842+6809				
	X	Ka	Q	
SNR after P-R	58.5	23.1	4.0	
effectiveness	△	◯	×	

4 Statistical Analysis of SVLBI P-R Input Catalogue

Histograms of the reference sources listed in section 3 are shown in Figure 1. The height of the red, blue and black bars show the number of the reference sources which is useful, not needed, and useless in P-R, respectively.

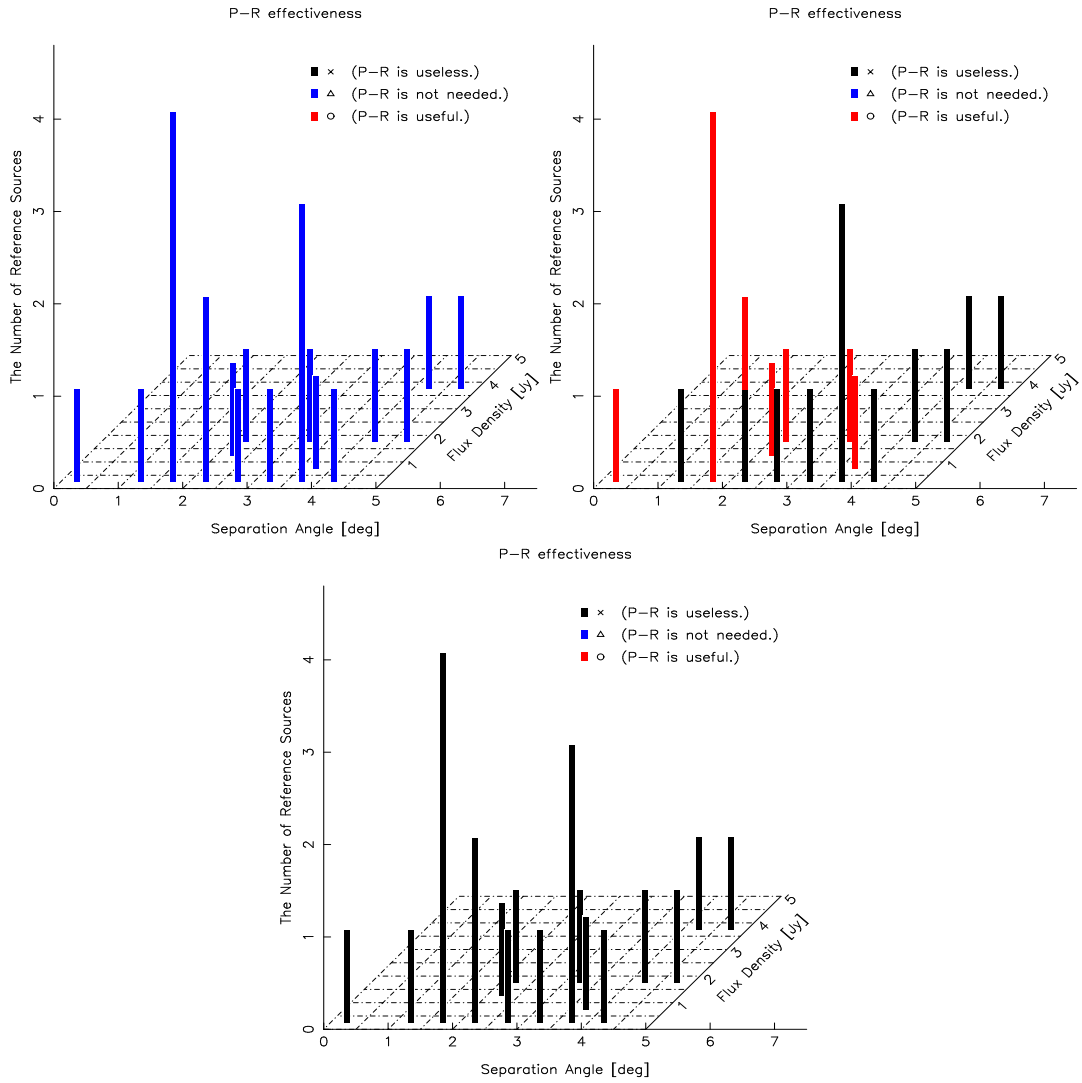

Figure 1: Histogram of the reference sources in the P-R input catalogue for weak GPS sources. The top left, right, and bottom drawing show the sources at 8, 22, and 43 GHz, respectively. The height of the red, blue and black bars show the number of the reference sources which is useful, not needed, and useless in P-R, respectively.

References